Sprint training attenuates myocyte hypertrophy and improves Ca^{2+} homeostasis in postinfarction myocytes

XUE-QIAN ZHANG,[1] YUK-CHOW NG,[2] TIMOTHY I. MUSCH,[4] RUSSELL L. MOORE,[5] R. ZELIS,[1,3] AND JOSEPH Y. CHEUNG[1,3]

Departments of [1]Medicine, [2]Pharmacology, and [3]Cellular and Molecular Physiology, Milton S. Hershey Medical Center, Pennsylvania State University, Hershey, Pennsylvania 17033; [4]Department of Anatomy and Physiology, Kansas State University, Manhattan, Kansas 66506; and [5]Department of Kinesiology, University of Colorado, Boulder, Colorado 80309

Zhang, Xue-Qian, Yuk-Chow Ng, Timothy I. Musch, Russell L. Moore, R. Zelis, and Joseph Y. Cheung. Sprint training attenuates myocyte hypertrophy and improves Ca^{2+} homeostasis in postinfarction myocytes. *J. Appl. Physiol.* 84(2): 544–552, 1998.—Myocytes isolated from rat hearts 3 wk after myocardial infarction (MI) had decreased Na^+/Ca^{2+} exchange currents ($I_{Na/Ca}$; 3 Na^+ out:1 Ca^{2+} in) and sarcoplasmic reticulum (SR)-releasable Ca^{2+} contents. These defects in Ca^{2+} regulation may contribute to abnormal contractility in MI myocytes. Because exercise training elicits positive adaptations in cardiac contractile function and myocardial Ca^{2+} regulation, the present study examined whether 6–8 wk of high-intensity sprint training (HIST) would ameliorate some of the cellular maladaptations observed in post-MI rats with limited exercise activity (Sed). In MI rats, HIST did not affect citrate synthase activities of plantaris muscles but significantly increased the percentage of cardiac α-myosin heavy chain (MHC) isoforms (57.2 ± 1.9 vs. 49.3 ± 3.5 in MI-HIST vs. MI-Sed, respectively; $P \leq 0.05$). At the single myocyte level, HIST attenuated cellular hypertrophy observed post-MI, as evidenced by reductions in cell lengths (112 ± 4 vs. 130 ± 5 μm in MI-HIST vs. MI-Sed, respectively; $P \leq 0.005$) and cell capacitances (212 ± 8 vs. 242 ± 9 pF in MI-HIST vs. MI-Sed, respectively; $P \leq 0.015$). Reverse $I_{Na/Ca}$ was significantly lower ($P \leq 0.0001$) in myocytes from MI-Sed rats compared with those from rats that were sham operated and sedentary. HIST significantly increased reverse $I_{Na/Ca}$ ($P \leq 0.05$) without affecting the amount of Na^+/Ca^{2+} exchangers (detected by immunoblotting) in MI myocytes. SR-releasable Ca^{2+} content, as estimated by integrating forward $I_{Na/Ca}$ during caffeine-induced SR Ca^{2+} release, was also significantly increased ($P \leq 0.02$) by HIST in MI myocytes. We conclude that the enhanced cardiac output and stroke volume in post-MI rats subjected to HIST are mediated, at least in part, by reversal of cellular maladaptations post-MI.

exercise training; excitation-contraction coupling; patch clamp; ventricular remodeling; cardiac hypertrophy

VENTRICLES that have survived significant myocardial infarction (MI) undergo many morphological, biochemical, cellular, and molecular adaptations that collectively contribute to progressive hemodynamic deterioration and the development of congestive heart failure. Deficits in cardiovascular function post-MI can be improved by dynamic aerobic exercise in humans (14, 15) and animal models (25–27). The cellular mechanisms underlying these training-induced improvements in cardiac function post-MI have not been elucidated. Reported cellular changes in myocytes isolated from hearts with healed MI include myocyte hypertrophy (1, 6, 40, 41), shift of myosin heavy chain (MHC) isoenzyme distribution from fast to slow isoforms (27), decreased densities of dihydropyridine binding sites (10, 40) and of both α- and β-adrenergic receptors (5, 36), depressed sarcolemmal (SL) Na^+-K^+-adenosinetriphosphatase (ATPase) and Na^+/Ca^{2+} exchange activities (11, 41), altered cytosolic free Ca^{2+} concentration ($[Ca^{2+}]_i$) dynamics during excitation-contraction (6, 39), depressed myocyte shortening (6, 23), and decreased sarcoplasmic reticulum (SR) Ca^{2+} contents (41). It is noteworthy that some of the MI-induced cellular maladaptations may potentially be reversed by exercise training. For example, in normal hearts, exercise training shifted MHC isoenzyme distribution from slow to fast forms (30), increased dihydropyridine-binding capacities in highly enriched cardiac SL vesicles (9), increased SL Na^+-K^+-ATPase activities (19), enhanced Ca^{2+} efflux-pathways (24), and improved myocyte contractile performances (24).

Recently, the potentially important role of Na^+/Ca^{2+} exchange in mediating Ca^{2+} entry during depolarization and subsequently triggering SR Ca^{2+} release to initiate contraction has been recognized (21, 29, 37). In addition, Ca^{2+} influx via reverse Na^+/Ca^{2+} exchange may serve to load the SR with Ca^{2+} for subsequent release (29). By directly modulating SR Ca^{2+} content and Ca^{2+} efflux pathways, Na^+/Ca^{2+} exchange may affect $[Ca^{2+}]_i$ dynamics (41) and thus excitation-contraction coupling (34). We have recently demonstrated, in myocytes isolated from hearts 3 wk post-MI, that whole cell Na^+/Ca^{2+} exchange current ($I_{Na/Ca}$) and SR Ca^{2+} contents (41), but not whole cell Ca^{2+} currents (40), were decreased compared within myocytes from sham-operated hearts (Sham). The present study was undertaken to evaluate whether high-intensity sprint training (HIST), an exercise-training program that we have previously shown to increase cardiac output and maximal stroke volume (SV_{max}) in rats with chronic MI (25), would restore $I_{Na/Ca}$ and SR Ca^{2+} contents toward normal levels and thus provide a cellular basis for the beneficial effects of exercise training on cardiac performance post-MI.

METHODS

Animal preparation and exercise-training protocol. To induce MI, the left main coronary artery of each anesthetized (3% halothane-97% O_2), intubated, and ventilated male Sprague-Dawley rat (weight ~300 g) was ligated 3–5 mm distal to its origin from the ascending aorta. In our previous studies (26) employing similar coronary artery ligation techniques, left ventricular (LV) infarct size, as determined

histologically, averaged 36 ± 3%. Sham operation was identical, except that the coronary artery was not occluded. All surviving rats received rat chow and water ad libitum and were maintained on a 12:12-h light-dark cycle. At 2 wk postoperation, all rats were introduced to running (0° grade, 10 m/min, 10 min/day, 5 days/wk) on a motor-driven treadmill (Precision Biomedical Systems, State College, PA). All sham-operated rats (n = 10) continued in this leisurely program (Sham-Sed) for another 7–9 wk before they were killed. At 3 wk postoperation, MI rats were randomly assigned to either a training (MI-HIST, n = 18) or a sedentary (MI-Sed, n = 16) group. MI-Sed rats participated in the same treadmill-walking program as Sham-Sed rats for 6–8 wk before they were killed. During the first week of training (*week 4* post-MI), MI-HIST rats ran five consecutive 1-min bouts daily, 5 days/wk, and each running bout was interspersed with 60 s of rest. Treadmill speed and grade were set at 66 m/min and 15°, respectively. During the second week of training (*week 5* post-MI), treadmill speed was progressively increased to 97 m/min. The treadmill grade and speed were then held constant for the remainder of the training period. We have previously shown that this HIST regimen resulted in significant increases in cardiac output and SV_{max} in post-MI rats (25). Use of HIST also circumvented potential problems with different degrees of exercise stress produced by endurance training.

LV myocyte isolation. After 6–8 wk of training (9–11 wk postoperation), rats were anesthetized with pentobarbital sodium (35 mg/kg body wt ip); their hearts were then excised for myocyte isolation. Myocytes were isolated from the septal and LV free wall portions of the myocardium, as previously described (6–8). The infarct scars in MI hearts were excised before the final enzymatic digestion step. Myocytes were allowed to adhere for 2 h to laminin-coated coverslips in 2 ml of medium 199 (pH 7.4; 95% air-5% CO_2; 37°C) before electrophysiological measurements were made (8, 40, 41). Patch-clamp studies were performed within 2–10 h of myocyte isolation. As in our previous studies (40, 41), myocytes that retained elongated shape and sharp cross striations, adhered to coverglass, and showed no membrane blebs were randomly chosen for electrophysiological measurements. Maximal lengths for myocytes were measured as described (6, 24, 38), except that the video camera used was a sequential scanning camera (TM 640 MOS; Pulnix America, Sunnyvale, CA), and distance calibration was performed with an Ealing high-resolution test target.

$I_{Na/Ca}$ measurements. Whole cell patch-clamp recordings were performed at 29°C, as described by Hamill et al. (16) and adapted by us for cardiac myocytes (40, 41). To isolate reverse $I_{Na/Ca}$ (3 Na^+ out:1 Ca^{2+} in), pipette solution consisted of (in mM) 100 Cs^+ glutamate, 20 NaCl, 1 $MgCl_2$, 30 *N*-2-hydroxyethylpiperazine-*N*′-2-ethanesulfonic acid, 2.5 Na_2ATP, 9 phosphocreatine, 0.1 1,4-dithiothreitol, and 30 U/ml creatine phosphokinase, pH 7.2. Free Ca^{2+} due to contaminant Ca^{2+} in pipette solution was 321 ± 9 nM, as measured fluorimetrically with fura 2 (8, 41). Myocytes were bathed in 0.6 ml of temperature (29°C)- and air-equilibrated external solution containing (in mM) 130 NaCl, 5 CsCl, 1.2 $MgSO_4$, 1.2 NaH_2PO_4, 1.8 $CaCl_2$, 20 *N*-2-hydroxyethylpiperazine-*N*′-2-ethanesulfonic acid, 10 glucose, 2.5 pyruvic acid, and 0.001 verapamil, pH 7.4. We have previously shown (41) that, by using these solutions, depolarization-induced steady-state outward currents possessed the following characteristics: *1*) increased with increasing extracellular Ca^{2+} concentration ($[Ca^{2+}]_o$) from 1.8 to 5.0 mM; *2*) decreased with decreasing intracellular Na^+ concentration ($[Na^+]_i$) from 25 to 5 mM; *3*) was abolished when $[Ca^{2+}]_i$ was reduced to zero by excess ethylene glycol-bis(β-aminoethyl ether)-*N*,*N*,*N*′,*N*′-tetraacetic acid (EGTA); *4*) was blocked by 5 mM Ni^{2+}; *5*) increased at more positive voltages; and *6*) decreased when $[Ca^{2+}]_i$ was lowered from 320 to 50 nM. These characteristics are most consistent with reverse $I_{Na/Ca}$.

Before myocyte stimulation, holding potential was switched from −70 to −40 mV to inactivate fast inward Na^+ current (40). Six conditioning pulses (from −40 to 0 mV, 300 ms, 1 Hz) were delivered before arrival of each test pulse (between −30 and +70 mV, 10-mV increments, 1,000 ms). After the last test pulse at +70 mV, the myocyte was held at −40 mV for 100 ms before being returned to holding potential of −70 mV. Reverse $I_{Na/Ca}$ was averaged from 700 to 1,000 ms of the test pulse. Myocyte capacitance (C_m) measurements and leakage current subtraction were performed as described previously (40, 41). Voltage-clamp experiments were performed by using an Axopatch 1-C amplifier (Axon Instruments, Foster City, CA) with a CV-4/100 headstage. Data acquisition (0.5 kHz) and analysis were by pClamp 5.5 software interfaced with TL-1 DMA analog-to-digital and digital-to-analog converter (Axon Instruments).

In some experiments, on the completion of $I_{Na/Ca}$ recordings, the bath in the chamber was drained to facilitate removal of the single myocyte in which $I_{Na/Ca}$ was measured; subsequently, MHC isoenzyme distribution was determined in that single cardiac myocyte.

Caffeine-induced SR Ca^{2+} release. SR-releasable Ca^{2+} content was estimated by measuring the time integral of forward $I_{Na/Ca}$ (3 Na^+ in:1 Ca^{2+} out) induced by caffeine exposure, as described by Callewaert et al. (4) and Zhang et al. (41). In these experiments, the pipette solution was similar to that used for reverse $I_{Na/Ca}$ measurements except that NaCl was reduced from 20 to 10 mM, thus making the final Na^+ concentration 15 mM. Holding potential was −70 mV, and verapamil was absent from the external solution. To ensure steady-state SR Ca^{2+} load, myocytes were exposed to identical trains of six conditioning pulses. At 200 ms after the last conditioning pulse, with membrane potential held at −70 mV, caffeine (5 mM) was applied by puffer superfusion (41). Currents were digitized at 0.5 kHz and collected for ~4 s.

Citrate synthase assays, MHC isoenzyme pattern and protein determinations, and Na^+/Ca^{2+} exchanger immunoblotting. Plantaris muscles were isolated, excessive nerve and connective tissue were removed, and the muscles were weighed before homogenization in 10 vol of ice-cold (0–2°C) potassium phosphate buffer (50 mM, pH 7.4 at 25°C). The homogenate was diluted 1:1 with homogenizing potassium phosphate buffer containing 0.2% bovine serum albumin, divided into 100-μl aliquots, quick-frozen in liquid N_2, and stored at −70°C. An aliquot of the diluted homogenate was frozen and thawed three times before it was assayed for citrate synthase activity at 25°C, as previously described (24, 33). Assays were linear with respect to time and dilution.

For analysis of MHC isoenzyme distributions, 500 μl of freshly isolated myocyte suspensions were centrifuged, and 500 μl of homogenization/extraction buffer (in mM: 10 tris(hydroxymethyl)aminomethane·HCl, 1 EDTA, 0.5 phenylmethylsulfonyl fluoride, pH 8.1 at room temperature) were added to the cell pellet. The homogenate was sonicated 3 × 15 s, an aliquot was taken for protein determination, and the remainder was stored at −70°C until it was used. Proteins were assayed by using a Bio-Rad DC protein assay kit (Bio-Rad, Hercules, CA). Myocyte suspension homogenates (1 μg/lane) were subjected to sodium dodecyl sulfate-polyacrylamide gel electrophoresis (SDS-PAGE) in 4–9% gradient gels (4°C) that were stained with silver to visualize MHC α- and β-isoenzymes as previously described (3). For analysis of single-myocyte MHC-isoenzyme distribution, a

myocyte attached to patch pipette was carefully lifted from the coverglass and placed in 50 µl of SDS-PAGE sample buffer containing 1% 2-mercaptoethanol. The tube containing the sample was sonicated for 3 × 15 s with a sonicator probe positioned immediately outside the tube. The entire tube contents were loaded onto a 4–9% gradient gel and MHC α- and β-isoenzymes were separated as described above. Protein molecular markers (Bio-Rad) were electrophoresed in parallel lanes. After being stained with silver, MHC isoenzyme bands were quantitated by laser densitometry (Molecular Dynamics, Sunnyvale, CA) and by using Quantity 1 (version 2) software (PDI Protein Databases, Huntington Station, NY).

For analysis of cardiac Na^+/Ca^{2+} exchanger, myocyte suspension homogenates (100 µg/lane) in SDS sample buffer [containing 10 mM *N*-ethylmaleimide (NEM) instead of 1% 2-mercaptoethanol] were applied to an 8.5% polyacrylamide gel, and proteins were separated by electrophoresis (31). Proteins from SDS-PAGE were transferred onto Immobilon-P membranes (Millipore, Bedford, MA). An antibody (1:1,000) against cardiac Na^+/Ca^{2+} exchange protein (π 11–13; SWant, Bellinzona, Switzerland), initially developed in the laboratory of K. D. Philipson (31), was used. Bound primary antibodies were detected with ^{125}I-goat anti-rabbit immunoglobulin G (DuPont NEN Research Products, Boston, MA), and immunoblots were subjected to autoradiography for 48 h. Autoradiograms were quantified by laser densitometry as described above.

Statistics. All results are expressed as means ± SE. In each experimental group (e.g., MI-Sed), myocytes isolated from some animals were used for $I_{Na/Ca}$ measurements, whereas other isolations were used for determinations of SR-releasable Ca^{2+}, percent α-MHC, or Na^+/Ca^{2+} exchange protein. It was not practicable to measure all of the parameters in any one myocyte isolation. Single between-group comparisons (e.g., cell length, citrate synthase activity, MI-Sed vs. MI-HIST) were made by using unpaired Student's *t*-tests. When more than two groups were involved (e.g., C_m, percent α-MHC isoenzyme, Sham-Sed vs. MI-Sed vs. MI-HIST), significance of differences among the means was determined by one-way analysis of variance (ANOVA). A priori comparisons of means of any two groups (e.g., MI-Sed vs. MI-HIST) were then performed by using *F*-tests as tests of significance. In experiments in which $I_{Na/Ca}$ measurements were made as a function of experimental group (Sham-Sed vs. MI-Sed vs. MI-HIST), voltage, and $[Ca^{2+}]_o$, three-way ANOVA of repeated measures was performed to determine significance of difference. A commercial software package (Statistical Analysis Systems) was used, and a mixed procedure was used. Post hoc paired comparisons were performed between Sham-Sed vs. MI-Sed and between MI-Sed vs. MI-HIST. In all analyses, a P of ≤ 0.05 was taken to be statistically signicant.

RESULTS

Effects of prior MI ± HIST on cell size and myosin isoenzyme distribution. We have previously demonstrated (6) that at 3 wk post-MI, myocytes have undergone hypertrophy, primarily an increase of ~10% in cell length, with little change in cell width. Myocyte hypertrophy post-MI was also reflected by a 13–15% increase in C_m (40, 41), an estimate of cell surface area. In the present study, C_m in MI-Sed myocytes was 25% larger than in Sham-Sed myocytes (Table 1). This suggests that myocyte hypertrophy not only persisted but might have progressed during the 9- to 11-wk post-MI period. In addition, cardiac MHC isoenzyme switched from the fast (α) to the slow (β) isoforms post-MI (Fig. 1; Table 1), similar to what we have reported previously in intact rat hearts with chronic infarction (27). HIST for 6–8 wk attenuated cell hypertrophy in MI myocytes, as evidenced by reduction of C_m to values observed in Sham-operated myocytes (Table 1; Sham-Sed vs. MI-HIST; not significant). Cell length significantly ($P \leq 0.005$) decreased from 130 ± 5 µm in MI-Sed myocytes (n = 24) to 112 ± 4 µm in MI-HIST myocytes (n = 22). In addition, HIST also effected a significant increase in relative MHC α-isoenzyme abundance in MI myocytes,

Table 1. *Effects of MI and HIST on selected cellular parameters*

	Sham-Sed	MI-Sed	MI-HIST
Single myocyte			
Myocyte capacitance, pF	194 ± 9 (25)	242 ± 9† (44)	212 ± 8* (49)
Myosin α-isoenzyme, %	94.0 ± 2.1 (12)	55.3 ± 2.0† (13)	88.6 ± 2.6* (14)
$I_{Na/Ca}$ time integral, pC/cell	ND	98.9 ± 6.5 (11)	162.0 ± 14.4* (9)
SR-releasable Ca^{2+}, fM/fF	ND	5.256 ± 0.565 (11)	7.597 ± 0.679* (9)
Myocyte suspension			
Myosin α-isoenzyme, %	71.2 ± 2.3 (5)	49.3 ± 3.5† (4)	57.2 ± 1.9* (5)
Na^+/Ca^{2+} exchanger protein, arbitrary units	1.125 ± 0.131 (9)	1.053 ± 0.130 (8)	1.236 ± 0.119 (9)

Values are means ± SE. In single myocyte measurements, nos. in parenthesis are nos. of cells, without regard to no. of cells contributed by each heart. MI, myocardial infarction; HIST, high-intensity sprint training; Sed, sedentary. In each experimental group, some myocyte isolations (hearts) were used for Na^+/Ca^{2+} exchange current ($I_{Na/Ca}$) measurements, while other isolations (hearts) were used for sarcoplasmic reticulum (SR)-releasable Ca^{2+}, %α-myosin heavy chain (MHC) or Na^+/Ca^{2+} exchange protein measurements. In myocyte suspension measurements, no. in parentheses is no. of cell isolations (hearts) studied. Relative myosin α-isoenzyme abundance was obtained from gels shown in Fig. 1. Apparent differences between %α-MHC measured in cell suspensions and single myocytes isolated from same animal groups [e.g., sham-operated sedentary rats (Sham-Sed)] were most likely caused by the very small amount of protein loading in single cell lanes (average myocyte protein content 5.7 ng; Ref. 41) when compared to cell suspension lanes (1 µg). A 30% β-MHC in a single Sham-Sed cardiac myocyte would correspond to ~0.3–0.4 ng of protein, at or below lower limit of resolution of silver-stained gel method (0.5–1.0 ng). This results in optical density of β-MHC band being close to background (Fig. 1, *lane 4* from *left*) and leads to artifactually high %α-MHC values in single Sham-Sed myocytes. By contrast, 50% β-MHC in single MI-Sed myocyte would correspond to 0.6–0.8 ng of protein, easily detectable on silver-stained gel (Fig. 1, *lane 5* from *left*). The much better signal-to-noise ratio of β-MHC band in single MI-Sed myocytes explains the good quantitative agreement between single myocyte and myocyte suspension measurements in this group of myocytes. Single MI-HIST myocytes have %β-MHC values between those of MI-Sed and Sham-Sed myocytes, as evidenced by stronger β-MHC band signal when compared to Sham-Sed myocyte (Fig. 1, *lane 6* from *left*). $I_{Na/Ca}$ time integrals were calculated from tracings shown in Fig. 5. SR-releasable Ca^{2+} values were normalized to myocyte capacitance. To convert coulombs to moles, charge was divided by Faraday's constant of 96,487 coulombs/equivalent, based on 3 Na^+ being exchanged for each Ca^{2+}. Amounts of Na^+/Ca^{2+} exchanger protein were obtained from immunoblots shown in Fig. 3. Tests of significance were performed as described in METHODS. ND, not done. *$P < 0.05$, MI-HIST vs. MI-Sed; †$P < 0.001$, MI-Sed vs. Sham-Sed.

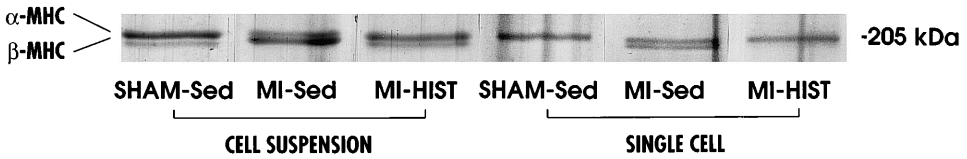

Fig. 1. High-intensity sprint training (HIST) increases myosin α-isoenzyme distribution in postinfarction myocytes. α-Myosin heavy chain (MHC) and β-MHC isoenzymes from left ventricular (LV) myocyte suspensions (*left* 3 lanes) and single LV myocytes (*right 3* lanes) were separated by gel electrophoresis and visualized by silver staining as described in METHODS. Note marked preponderance of α-isoenzyme of MHC in myocytes from Sham-operated hearts. Surgically induced myocardial infarction (MI) shifts MHC from α- to β-isoenzymes in sedentary (Sed) rats, but HIST restores MHC isoenzyme distribution toward that observed in Sham-operated and sedentary (Sham-Sed) rats. Note also in single myocyte studies (*right* 3 lanes), protein band corresponding to MHC β-isoenzyme is barely visible in Sham-Sed and MI-HIST myocytes but is much more prominent in MI-Sed myocytes. See also Table 1 legend.

although not quite to levels observed in myocytes isolated from Sham-operated hearts (Fig. 1, Table 1). Similar to our previous conclusions (25) that HIST produced a significant increase in maximal aerobic capacity, but not an increase in the oxidative enzyme capacity of skeletal muscles involved in locomotion, plantaris muscle citrate synthase activity in MI-HIST rats (23.2 ± 2.7 μmol·min^{-1}·g wet wt^{-1}, $n = 4$) was not different from that in MI-Sed rats (22.1 ± 4.6 μmol·min^{-1}·g wet wt^{-1}, $n = 3$).

Effects of prior MI ± HIST on reverse $I_{Na/Ca}$. Figure 2*A* shows the steady-state reverse $I_{Na/Ca}$ measured at various membrane potentials, at 29°C and 1.8 mM $[Ca^{2+}]_o$, in Sham-Sed, MI-Sed, and MI-HIST myocytes. In agreement with our previous observations (41), reverse $I_{Na/Ca}$ was lower in myocytes isolated from post-MI hearts compared with Sham-operated hearts (Fig. 2*A*). Importantly, reverse $I_{Na/Ca}$ in MI-HIST myocytes was higher than in MI-Sed myocytes, whether $[Ca^{2+}]_o$ was at 1.8 (Fig. 2*A*) or 5.0 mM (Fig. 2*B*). ANOVA (Table 2) confirmed a significant group effect (Sham-Sed vs. MI-Sed vs. MI-HIST). In all three groups, depolarization to more positive membrane potentials increased the absolute magnitude of reverse $I_{Na/Ca}$ (significant voltage effect; Table 2), as did increasing $[Ca^{2+}]_o$ from 1.8 to 5.0 mM (significant $[Ca^{2+}]_o$ effect, Table 2). Finally, the three-way group × voltage × $[Ca^{2+}]_o$ interaction was highly significant, suggesting that increasing $[Ca^{2+}]_o$ significantly affected the inherent differences in reverse $I_{Na/Ca}$ among Sham-Sed, MI-Sed, and MI-HIST myocytes across the voltages tested.

To further test for significant differences in reverse $I_{Na/Ca}$ between Sham-Sed and MI-Sed and between MI-Sed and MI-HIST myocytes, we performed post hoc analysis (Table 2). In agreement with our previous studies (41), reverse $I_{Na/Ca}$ was lower in MI-Sed myocytes compared with Sham-Sed myocytes (significant group effect; Table 2), and the inherent differences were amplified with depolarization and with increasing $[Ca^{2+}]_o$ (significant group × voltage × $[Ca^{2+}]_o$ effect; Table 2). HIST for 6–8 wk significantly increased reverse $I_{Na/Ca}$ in MI myocytes (significant group effect; Table 2). The inherent differences in reverse $I_{Na/Ca}$ between MI-Sed and MI-HIST myocytes were increased at more positive voltages (significant group × voltage effect; Table 2) but not by elevating $[Ca^{2+}]_o$ (insignificant group × $[Ca^{2+}]_o$ effect and insignificant three-way interaction; Table 2).

Effects of prior MI ± HIST on Na^+/Ca^{2+} exchanger abundance. To further elucidate the mechanisms by which HIST increased reverse $I_{Na/Ca}$ in myocytes isolated from MI hearts, we performed immunoblots of

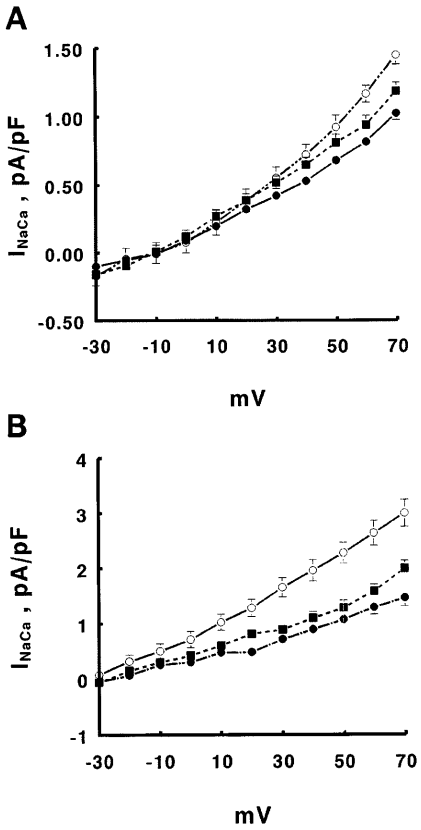

Fig. 2. Current-voltage relationships of Na/Ca^{2+} exchange current ($I_{Na/Ca}$) in Sham-Sed, MI-Sed, and MI-HIST myocytes. Steady-state $I_{Na/Ca}$ at each test potential was measured as described in METHODS. *A*: means ± SE for 15 Sham-Sed (○), 15 MI-Sed (●), and 16 MI-HIST (■) myocytes incubated at 1.8 mM extracellular Ca^{2+} concentration ($[Ca^{2+}]_o$). Free Ca^{2+} in pipette solution was ~320 nM. *B*: means ± SE for 11 Sham-Sed (○), 18 MI-Sed (●), and 19 MI-HIST (■) myocytes incubated at 5.0 mM $[Ca^{2+}]_o$ are shown. Error bars are not shown if they fall within boundaries of symbol. Results of 3-way analysis of variance are shown in Table 2.

Table 2. *ANOVA main effects and post hoc paired comparisons of* $I_{Na/Ca}$

Main Effects	*P*
Group (Sham-Sed vs. MI-Sed vs. MI-HIST)	0.0001
Voltage	0.0001
$[Ca^{2+}]_o$ (1.8 vs. 5.0 mM)	0.0001
Group × voltage	0.0001
Group × $[Ca^{2+}]_o$	0.0001
Group × voltage × $[Ca^{2+}]_o$	0.0001
Post hoc paired comparisons	
Sham-Sed vs. MI-Sed	
Group	0.0001
Group × voltage	0.0001
Group × $[Ca^{2+}]_o$	0.0001
Group × voltage × $[Ca^{2+}]_o$	0.0001
MI-Sed vs. MI-HIST	
Group	0.0500
Group × voltage	0.0005
Group × $[Ca^{2+}]_o$	0.2895
Group × voltage × $[Ca^{2+}]_o$	0.1478

Data are from Fig. 2. $[Ca^{2+}]_o$, extracellular Ca^{2+} concentration; ANOVA, analysis of variance; *P*, probability of type I error. For clarity of presentation, significant voltage ($P<0.0001$) and $[Ca^{2+}]_o$ ($P<0.0001$) effects in post hoc analysis are not included.

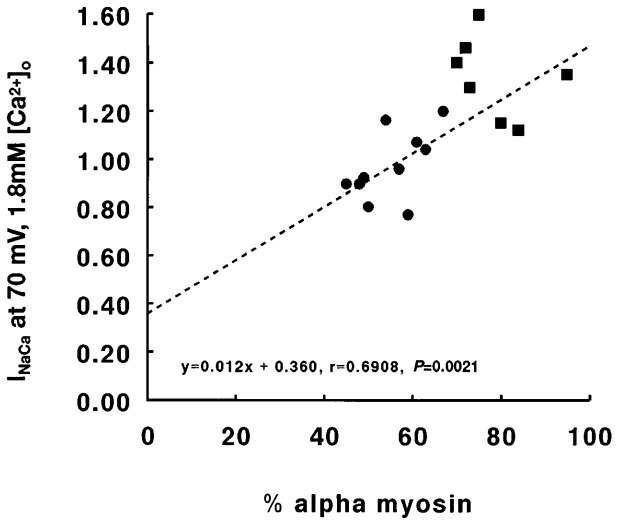

Fig. 4. Relationship between $I_{Na/Ca}$ and %myosin α-isoenzyme in single MI myocytes. Steady-state $I_{Na/Ca}$ at +70 mV and 1.8 mM $[Ca^{2+}]_o$ were measured in 10 MI-Sed (●) and 7 MI-HIST (■) myocytes, followed by %myosin α-isoenzyme determinations (Fig. 1) in same myocytes. Linear regression analysis shows that regression line fits significantly ($P = 0.002$) better than horizontal line at mean (single-mean model).

isolated cardiac myocyte homogenates probed with antibody to the Na^+/Ca^{2+} exchanger (Fig. 3). Using nonreducing (10 mM NEM) gel conditions, we detected a major band of apparent molecular weight of 160 kDa and a minor band at 120 kDa. This is similar to the results reported by Philipson et al. (31). There were no significant differences in the amounts of Na^+/Ca^{2+} exchanger protein among Sham-Sed, MI-Sed, and MI-HIST myocytes (Fig. 3; Table 1) . When autoradiographical signals corresponding to the Na^+/Ca^{2+} exchanger (160- and 120-kDa bands) from MI-Sed and MI-HIST myocytes were expressed relative to those from Sham-Sed myocytes (arbitrarily defined as 1.0) ran on the same gel, the means ± SE for MI-Sed ($n = 8$) and MI-HIST ($n = 9$) myocytes were 0.912 ± 0.131 and 1.020 ± 0.102, respectively ($P = 0.6583$).

Relationship between reverse $I_{Na/Ca}$ *and myosin isoenzyme distribution in MI myocytes.* To examine whether the increase in reverse $I_{Na/Ca}$ in a single MI-HIST myocyte was caused by specific effects of HIST and not by random variation, we measured relative percentage of α-MHC isoenzyme in the same single myocyte (Fig. 1, Table 1) after $I_{Na/Ca}$ measurements were completed. Figure 4 shows the relationship between reverse $I_{Na/Ca}$ (measured at +70 mV, 29°C, and 1.8 mM $[Ca^{2+}]_o$) and relative percentage of α-MHC in individual MI-Sed and MI-HIST myocytes. Note that in myocytes isolated from hearts with chronic MI, reverse $I_{Na/Ca}$ generally increased as relative percentage of α-MHC increased. Indeed, linear regression analysis of combined data from MI-Sed and MI-HIST myocytes showed a significant correlation ($P = 0.002$) between reverse $I_{Na/Ca}$ and relative percentage of α-MHC (Fig. 4). In addition, in this group of 17 myocytes, there was little overlap between MI-Sed and MI-HIST myocytes in relative percentage of α-MHC ($P < 0.0001$).

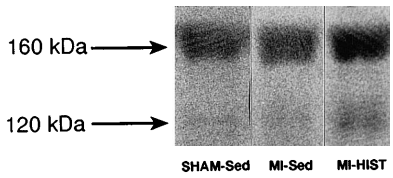

Fig. 3. Immunoblots of Na^+/Ca^{2+} exchanger protein. Proteins in myocyte suspension homogenates (100 μg/lane) were separated by gel electrophoresis, transferred to Immobilon-P membranes, and Na^+/Ca^{2+} exchanger was identified by immunoblotting, as described in METHODS. Note prominence of polypeptide band at 160 kDa under our nonreducing gel conditions, in agreement with Philipson et al. (32). Polypeptide bands at both 160 and 120 kDa were quantitated by laser densitometry (METHODS), and results are shown in Table 1.

Effects of prior MI ± HIST on caffeine-induced SR Ca^{2+} *release.* Application of 5 mM caffeine for 2.4 s on a MI-Sed myocyte at −70 mV and 5 mM $[Ca^{2+}]_o$ caused a large inward current that rapidly returned to baseline (Fig. 5*B*). This inward current represented forward Na^+/Ca^{2+} exchange (3 Na^+ in:1 Ca^{2+} out) operating to extrude SR Ca^{2+} released by caffeine. We (41) and others (4) have shown that under our experimental conditions, the time integral of the caffeine-induced inward current was an estimate of SR-releasable Ca^{2+} of the myocyte. Both $I_{Na/Ca}$ time integral and SR-releasable Ca^{2+} (normalized to cell size) were significantly larger in MI-HIST (Fig. 5*C*) than in MI-Sed (Fig. 5*B*) myocytes (Table 1). It should be emphasized that the SR Ca^{2+} contents represented steady-state values, because both MI-Sed and MI-HIST myocytes were subjected to identical trains of conditioning pulses (Fig. 5*A*).

DISCUSSION

Our study is the first to demonstrate potential cellular mechanisms by which a program of exercise train-

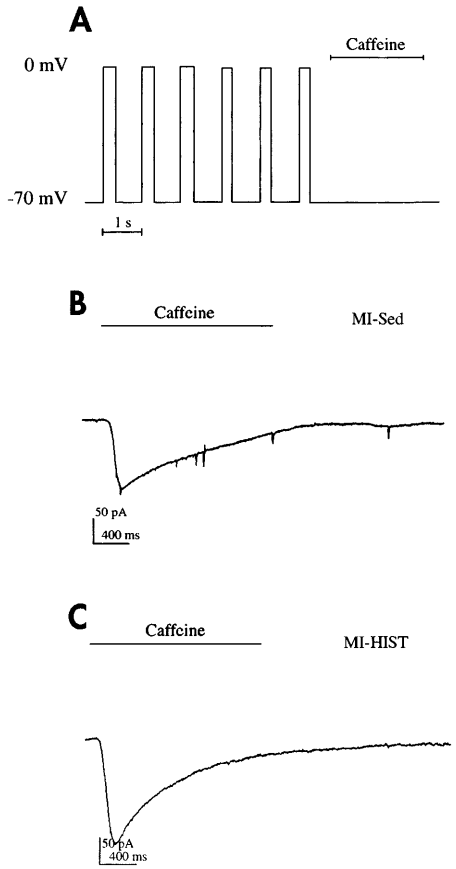

Fig. 5. Estimation of sarcoplasmic reticulum (SR)-releasable Ca^{2+} content in post-MI myocytes. Myocytes were incubated with 5.0 mM $[Ca^{2+}]_o$ at 29°C and were voltage-clamped at −70 mV. *A*: 200 ms after 6th conditioning pulse (from −70 to 0 mV, 300 ms, 1 Hz), caffeine (5 mM) was "puffed" onto myocyte for 2.4 s (index bar). *B*: large transient inward current caused by caffeine-induced SR Ca^{2+} release was observed in MI-Sed myocyte. We (41) and others (4) have shown that this current represents Na^+ entry caused by Ca^{2+} extrusion by Na^+/Ca^{2+} exchange (3 Na^+ in:1 Ca^{2+} out), and that the time integral of this inward current provided an estimate of SR-releasable Ca^{2+}. *C*: response by MI-HIST myocyte to caffeine pulse. Note that $I_{Na/Ca}$ time integral of MI-Sed myocyte is less than that of MI-HIST myocyte. Composite data are shown in Table 1.

ing instituted shortly after recovery from acute MI leads to improvement in overall cardiac performance. We have previously shown in conscious and instrumented rats with moderate-size (~35%) healed LV infarcts that 6 wk of HIST (25), but not 8–10 wk of endurance training (26, 27), increased maximal cardiac output without changing heart rate, thus indicating an increase in SV_{max}. While systemic factors (central cardioregulatory and peripheral vascular adaptations, and so forth) likely contributed to HIST-induced improvement in cardiac performance in rats with chronic MI, cellular adaptations to HIST may be equally important to improved myocardial function in post-MI hearts. For cellular events involved in excitation-contraction coupling in cardiac myocytes, reported singular effects of MI are often opposite in direction to those of exercise training (6, 9, 11, 12, 19, 20, 22–24, 27, 30, 35, 39–41). This suggests that exercise training may reverse some of the deleterious cellular changes induced by MI.

The intensity of our sprint training protocol appropriately raises some concerns relating to its potential clinical implications for post-MI patients. We chose the HIST regimen for the present study because, within a reasonable period (6 wk) of training, it effected a statistically significant SV_{max} increase in post-MI hearts (25) whereas 8–10 wk of moderate endurance running only resulted in a "trend" ($P = 0.08$) in cardiac output improvement (26, 27). In addition, HIST circumvents potential problems with different degrees of exercise stress produced by endurance training. Finally, our previous (25) and present experiments clearly demonstrated that HIST did not cause harmful or even fatal effects that may occur when rats with moderate-sized LV infarcts were subjected to a strenuous exercise program. Thus, with our working hypothesis that exercise training improves cardiac function post-MI by effecting cellular changes in addition to myocardial adaptation, we felt it was more fruitful and expeditious to focus on HIST. Whether a less strenuous exercise regimen (but probably of more protracted duration), which is clinically more relevant, can effect cellular adaptations similar to those induced by HIST is speculative at present.

The first major finding is that HIST attenuated cellular hypertrophy observed in MI-Sed myocytes. When compared with MI-Sed myocytes, the ~12% reduction in C_m was almost matched by the ~14% decrease in myocyte length in MI-HIST myocytes. This suggests that HIST reduced myocyte hypertrophy primarily by decreasing cell length. We have previously shown (6) that myocytes isolated from hearts with chronic LV infarct underwent ~10% increase in cell length with no change in cell diameter, a characteristic of volume-overload hypertrophy (1) as opposed to pressure-overload hypertrophy (38). It is interesting to speculate that by directly affecting cell-length increases in postinfarction myocytes, HIST may minimize ventricular remodeling post-MI (1) and thus prevent development of dilated cardiomyopathy.

The second finding is that, like post-MI endurance training (27), HIST produced a significant shift in the cardiac myosin isoenzyme composition (from β- to α-) in MI myocytes (Fig. 1, Table 1). This shift in myosin isoenzyme distribution was detectable at the single myocyte level (Fig. 1). The training-induced reversal in myosin isoenzyme composition (from slower to fast myosin ATPase) may account for some of the improvements in cardiac pump function (increased cardiac output and SV_{max}) in MI rats.

Recent studies increasingly support the important roles for Na^+/Ca^{2+} exchange in Ca^{2+} homeostasis in cardiac myocytes, not only in its traditional role of being the major Ca^{2+} efflux pathway during diastole (2) but also in its dual role in triggering SR Ca^{2+} release during systole (21, 37) and loading the SR with Ca^{2+} for subsequent release (29). In addition, we have reported significant $[Ca^{2+}]_i$-independent decreases in reverse $I_{Na/Ca}$ in cardiac myocytes isolated from rats 3 wk after MI (41). This is in agreement with depressed Na^+-dependent Ca^{2+} uptake in SL vesicles isolated from rat

hearts 4, 8, and 16 wk post-MI (11). Decreased Na^+/Ca^{2+} exchange activity may simultaneously account for the lower systolic and higher diastolic $[Ca^{2+}]_i$ observed in myocytes from hearts with chronic MI (39), as we have explained elsewhere (41). Thus the third major finding of the present study is that HIST significantly increased reverse $I_{Na/Ca}$ in MI myocytes, although not back to the levels measured in cardiac myocytes from Sham-Sed rats (Fig. 2; Table 2). Increased reverse $I_{Na/Ca}$ in MI-HIST myocytes may provide more SR Ca^{2+} for release (29), increase the gain (ratio of trigger Ca^{2+} to that released from the SR) of SR Ca^{2+} release channels (34), and enhance Ca^{2+} influx at more positive potentials reached during normal depolarization to increase the Ca^{2+} trigger for SR Ca^{2+} release (21, 37). On the other hand, increased forward $I_{Na/Ca}$ may result in more Ca^{2+} extrusion in MI-HIST myocytes during the relaxation phase of the contraction cycle (2). All these potential mechanisms would act in concert to restore toward normal the $[Ca^{2+}]_i$ dynamics during excitation-contraction. Because $[Ca^{2+}]_i$ occupies a central role in excitation-contraction coupling in cardiac myocytes, restoration of $[Ca^{2+}]_i$ transients toward normal may represent a major cellular mechanism by which HIST increased SV_{max} observed in rats with chronic MI (25).

To maximize $I_{Na/Ca}$ differences among the three experimental groups (41), the pipette solution (Ca^{2+} concentration = 320 nM) used in our present study was designed not to contain Ca^{2+}-EGTA buffer. Thus one simple explanation can be that differences in reverse $I_{Na/Ca}$ among Sham-Sed, MI-Sed, and MI-HIST myocytes were caused by differences in $[Ca^{2+}]_i$ among the three groups. It should be noted, however, that when Ca^{2+}-EGTA buffers were used to "clamp" $[Ca^{2+}]_i$ at 50 nM, significant differences in $I_{Na/Ca}$ were still present between Sham and MI myocytes (41), indicating $[Ca^{2+}]_i$-independent mechanisms of decreased Na^+/Ca^{2+} exchange activities in MI myocytes. In addition, exercise training (albeit endurance treadmill running) has been shown to decrease the Michaelis constant for Ca^{2+} of cardiac Na^+/Ca^{2+} exchange in isolated SL vesicles (35), indicating Ca^{2+}-independent modulation of Na^+/Ca^{2+} exchange activity by exercise training. Finally, resting $[Ca^{2+}]_i$ values were found to be similar between Sham and MI myocytes (6, 39) and between Sham and exercised-trained (endurance treadmill running) myocytes (20, 24) in rats. This last observation suggests that the cytoplasmic domain of the Na^+/Ca^{2+} exchanger was likely exposed to similar $[Ca^{2+}]_i$ in Sham-Sed, MI-Sed, and MI-HIST myocytes in the resting state.

Despite different magnitudes of Na^+/Ca^{2+} exchange current observed in Sham-Sed, MI-Sed, and MI-HIST myocytes (Fig. 2, Table 2), immunoblots did not detect significantly different amounts of Na^+/Ca^{2+} exchange protein among the three groups of myocytes (Fig. 3, Table 1). One explanation is that Western blots may not have the resolution to detect small changes in Na^+/Ca^{2+} exchange protein levels induced by MI or HIST, although $I_{Na/Ca}$ differences were demonstrated by the more sensitive electrophysiological techniques. Alternatively, MI and/or HIST may alter the activity of existing Na^+/Ca^{2+} exchange units. It is well-known that $I_{Na/Ca}$ is modulated by $[Na^+]_i$ and $[Ca^{2+}]_i$ (18), cellular ATP levels (17), pH (13), and phospholipid environment (32). Molecular studies of cardiac Na^+/Ca^{2+} exchangers also revealed cytoplasmic domains (calmodulin-like binding domain, Ca^{2+} binding sites) that can potentially be involved in regulation of Na^+/Ca^{2+} exchange activity (28). Our present studies did not go into sufficient detail to evaluate which of these known regulatory mechanisms of Na^+/Ca^{2+} exchange activity was affected by MI or HIST.

Within the subset of myocytes isolated from rat hearts with chronic MI, both chronic endurance training (27) and HIST (Table 1) significantly increased the α-MHC isoenzyme distribution in myocyte-suspension homogenates compared with that measured in sedentary controls. Thus, at the cellular level, this shift of relative percentage of α-MHC may be taken as an indicator of the trained state in MI rats. It is thus reassuring that in randomly chosen single MI myocytes in which both reverse $I_{Na/Ca}$ and α-MHC isoenzyme abundance were measured, higher $I_{Na/Ca}$ observed in MI-HIST myocytes was associated with a higher relative percentage of α-MHC (Fig. 4). This suggests that, despite the practical limitation inherent in electrophysiological experiments because only a small number of myocytes from a given heart could be examined in any given experiment, random sampling yielded results that were likely representative of the population. This is because *1*) the percentage of α-MHC present in single MI-HIST myocytes did not significantly ($P < 0.0001$) overlap with that in single MI-Sed myocytes and *2*) higher $I_{Na/Ca}$ in a single and randomly selected myocyte isolated from MI-HIST rat was associated with increase in percentage of α-MHC (Fig. 4), a cellular marker of the trained state.

We have previously shown that SR-releasable Ca^{2+} was lower in myocytes isolated from 3-wk MI hearts, and we attributed the deficit to decreased SR Ca^{2+}-ATPase amounts and/or activities, reduced amount or volume of SR per myocyte, and/or increased SR Ca^{2+} leak (41). Decreased SR-releasable Ca^{2+} content in MI myocytes would lower systolic $[Ca^{2+}]_i$ by reducing amount of Ca^{2+} available for release and decreasing the "gain" of SR Ca^{2+} release channels. Because HIST enhanced reverse $I_{Na/Ca}$ in MI myocytes, one functional consequence may be increased SR Ca^{2+} filling by reverse $I_{Na/Ca}$, leading to significantly larger SR Ca^{2+} content in MI-HIST myocytes. Thus the fourth major finding of the present study is that HIST significantly increased SR Ca^{2+} content in myocytes from post-MI hearts (Fig. 5, Table 1). Theoretically, HIST may improve SR Ca^{2+} content by *1*) increased Ca^{2+} influx via Ca^{2+} current (9); *2*) increased Ca^{2+} influx by reverse $I_{Na/Ca}$ (Fig. 2); *3*) increased SR Ca^{2+} uptake (22, 30); and *4*) decreased SR Ca^{2+} leak. Elucidation of which of these mechanisms accounted for the observed increases in SR Ca^{2+} content in MI-HIST myocytes would require further study, but HIST-induced increases in reverse $I_{Na/Ca}$ (Fig. 2) could certainly play a role.

In summary, we have shown that HIST attenuated at least several cellular maladaptations: cellular hypertrophy, myosin isoenzyme shifts, reduced Na^+/Ca^{2+} exchange activity, and decreased SR Ca^{2+} contents in myocytes from rat hearts with a moderate-size LV infarct. We hypothesize that, in post-MI rats, improvements in Ca^{2+} homeostatic pathways by HIST form the cellular basis of enhancement of cardiac performance.

We thank Dr. Kenneth D. Philipson for many helpful suggestions, Beverly Bell for assistance in preparation of the manuscript, and Anne Pruznak for expert technical assistance.

This work was supported in part by National Institutes of Health Grants DK-46778, HL-39723, HL-40306, HL-44146, and AG-11535 and by an American Heart Association-Pennsylvania Affiliate Grant-in-Aid.

Address for reprint requests: J. Y. Cheung, Div. of Nephrology, M. S. Hershey Medical Center, Hershey, PA 17033.

Received 28 April 1997; accepted in final form 17 October 1997.

REFERENCES

1. **Anversa, P., C. Beghi, Y. Kikkawa, and G. Olivetti.** Myocardial infarction in rats. Infarct size, myocyte hypertrophy, and capillary growth. *Circ. Res*. 58: 26–37, 1986.
2. **Bassani, R. A., J. W. M. Bassani, and D. M. Bers.** Mitochondrial and sarcolemmal Ca^{2+} transport reduce $[Ca^{2+}]_i$ during caffeine contractures in rabbit cardiac myocytes. *J. Physiol. (Lond.)* 453: 591–608, 1992.
3. **Book, C.-B. S., R. L. Moore, A. Semanchik, and Y.-C. Ng.** Cardiac hypertrophy aleters expression of Na^+, K^+-ATPase subunit isoforms at mRNA and protein levels in rat myocardium. *J. Mol. Cell. Cardiol*. 26: 591–600, 1994.
4. **Callewaert, G., L. Cleeman, and M. Morad.** Caffeine-induced Ca^{2+} release activates Ca^{2+} extrusion via Na^+-Ca^{2+} exchanger in cardiac myocytes. *Am. J. Physiol*. 257 (*Cell Physiol*. 26): C147–C152, 1989.
5. **Cheng, W., J. Coupet, P. Li, K. Reiss, C. V. Homcy, J. M. Capasso, L. G. Meggs, and P. Anversa.** Coronary artery constriction in rats affects the activation of alpha-1 adrenergic receptors in cardiac myocytes. *Cardiovasc. Res*. 28: 1070–1082, 1994.
6. **Cheung, J. Y., T. I. Musch, H. Misawa, A. Semanchick, M. Elensky, R. V. Yelamarty, and R. L. Moore.** Impaired cardiac function in rats with healed myocardial infarction: cellular vs. myocardial mechanisms. *Am. J. Physiol*. 266 (*Cell Physiol*. 35): C29–C36, 1994.
7. **Cheung, J. Y., I. G. Thompson, and J. V. Bonventre.** Effects of extracellular calcium removal and anoxia on isolated rat myocytes. *Am. J. Physiol*. 243 (*Cell Physiol*. 12): C184–C190, 1982.
8. **Cheung, J. Y., D. L. Tillotson, R. V. Yelamarty, and R. C. Scaduto, Jr.** Cytosolic free calcium concentration in individual cardiac myocytes in primary culture. *Am. J. Physiol*. 256 (*Cell Physiol*. 25): C1120–C1130, 1989.
9. **Diffee, G. M., and G. F. Tibbits.** Dihydropyridine binding to myocardial sarcolemma: adaptations to exercise (Abstract). *Clin. Physiol*. 5: 29, 1985.
10. **Dixon, I. M. C., T. Hata, and N. S. Dhalla.** Nitrendipine binding in congestive heart failure due to myocardial infarction. *Circ. Res*. 66: 782–788, 1990.
11. **Dixon, I. M. C., T. Hata, and N. S. Dhalla.** Sarcolemmal calcium transport in congestive heart failure due to myocardial infarction in rats. *Am. J. Physiol*. 262 (*Heart Circ. Physiol*. 31): H1387–H1394, 1992.
12. **Dixon, I. M. C., T. Hata, and N. S. Dhalla.** Sarcolemmal Na^+-K^+-ATPase activity in congestive heart failure due to myocardial infarction. *Am. J. Physiol*. 262 (*Cell Physiol*. 31): C664–C671, 1992.
13. **Doering, A. E., and W. J. Lederer.** The mechanism by which cytoplasmic protons inhibit the sodium-calcium exchanger in guinea-pig heart cells. *J. Physiol. (Lond.)* 466: 481–499, 1993.
14. **Ehsani, A. A., G. W. Heath, J. M. Hagberg, B. E. Sobel, and J. O. Holloszy.** Effects of 12 months of intense exercise training on ischemic ST-segment depression in patients with coronary artery disease. *Circulation* 64: 1116–1124, 1981.
15. **Hagberg, J. M., A. A. Ehsani, and J. O. Holloszy.** Effect of 12 months of intense exercise training on stroke volume in patients with coronary artery disease. *Circulation* 67: 1194–1199, 1983.
16. **Hamill, O. P., A. Marty, E. Neher, B. Sakman, and F. Sigworth.** Improved patch-clamp techniques for high resolution current recording from cells and cell-free membrane patches. *Pflügers Arch*. 391: 85–100, 1981.
17. **Hilgemann, D. W., and A. Collins.** Mechanisms of cardiac Na^+-Ca^{2+} exchange current stimulation by MgATP: possible involvement of aminophospholipid translocase. *J. Physiol. (Lond.)* 454: 59–82, 1992.
18. **Kimura, J., A. Noma, and H. Irisawa.** Na-Ca exchange current in mammalian heart cells. *Nature* 319: 596–597, 1986.
19. **Kjeldsen, K., P. Bjerregaard, E. A. Richter, P. E. Thomsen, and A. Norgaard.** Na^+-K^+-ATPase concentration in rodent and human heart skeletal muscle: apparent relation to muscle performance. *Cardiovasc. Res*. 22: 95–100, 1988.
20. **Laughlin, M. H., M. E. Schaeffer, and M. Sturek.** Effect of exercise training on intracellular free Ca^{2+} transients in ventricular myocytes of rats. *J. Appl. Physiol*. 73: 1441–1448, 1992.
21. **Levi, A. J., K. W. Spitzer, O. Kohmoto, and J. H. B. Bridge.** Depolarization-induced Ca entry via Na-Ca exchange triggers SR release in guinea pig cardiac myocytes. *Am. J. Physiol*. 266 (*Heart Circ. Physiol*. 35): H1422–H1433, 1994.
22. **Levine, S. N., and G. T. Kinasewitz.** Exercise conditioning increases rat myocardial calcium uptake. *J. Appl. Physiol*. 60: 1673–1679, 1986.
23. **Meggs, L. G., J. Coupet, H. Huang, W. Cheng, P. Li, J. M. Capasso, C. J. Homcy, and P. Anversa.** Regulation of angiotensin II receptors on ventricular myocytes after myocardial infarction in rats. *Circ. Res*. 72: 1149–1162, 1993.
24. **Moore, R. L., T. I. Musch, R. V. Yelamarty, R. C. Scaduto, Jr., A. M. Semanchick, M. Elensky, and J. Y. Cheung.** Chronic exercise alters contractility and morphology or isolated rat cardiac myocytes. *Am. J. Physiol*. 264 (*Cell Physiol*. 33): C1180–C1189, 1993.
25. **Musch, T. I.** Effects of sprint training on maximal stroke volume of rats with a chronic myocardial infarction. *J. Appl. Physiol*. 72: 1437–1444, 1992.
26. **Musch, T. I., R. L. Moore, D. J. Leathers, A. Bruno, and R. Zelis.** Endurance training in rats with chronic heart failure induced by myocardial infarction. *Circulation* 74: 431–441, 1986.
27. **Musch, T. I., R. L. Moore, P. G. Smaldone, M. Riedy, and R. Zelis.** Cardiac adaptations to endurance training in rats with chronic myocardial infarction. *J. Appl. Physiol*. 66: 712–719, 1989.
28. **Nicoll, D. A., S. Longoni, and K. D. Philipson.** Molecular cloning and functional expression of the cardiac sarcolemmal Na^+-Ca^{2+} exchanger. *Science* 250: 562–565, 1990.
29. **Nuss, H. B., and S. R. Houser.** Sodium-calcium exchange-mediated contractions in feline ventricular myocytes. *Am. J. Physiol*. 263 (*Heart Circ. Physiol*. 32): H1161–H1169, 1992.
30. **Pagani, E. G., and R. J. Solars.** Coordination of cardiac myofibrillar and sarcotubular activities in rats exercised by swimming. *Am. J. Physiol*. 247 (*Heart Circ. Physiol*. 16): H909–H915, 1984.
31. **Philipson, K. D., S. Longoni, and R. Ward.** Purification of the cardiac Na^+-Ca^{2+} exchange protein. *Biochim. Biophys. Acta* 945: 298–306, 1988.
32. **Philipson, K. D., and R. Ward.** Effects of fatty acids on Na^+ and Ca^{2+} permeability of cardiac sarcolemmal vesicles. *J. Biol. Chem*. 260: 9666–9671, 1985.
33. **Shepherd, D., and P. B. Garland.** Citrate synthase from rat liver. *Methods Enzymol*. 13: 11–13, 1969.
34. **Stern, M. D.** Theory of excitation-contraction coupling in cardiac muscle. *Biophys. J*. 63: 497–517, 1992.
35. **Tibbits, G. F., H. Kasihara, and K. O'Reilly.** Na^+-Ca^{2+} exchange in cardiac sarcolemma: modulation of Ca^{2+} affinity by exercise. *Am. J. Physiol*. 256 (*Cell Physiol*. 25): C638–C643, 1989.
36. **Vatner, D. E., M. A. Young, D. R. Knight, and S. F. Vatner.** β-receptors and adenylate cyclase: comparison of nonischemic,

ischemic, and postmortem tissue. *Am. J. Physiol.* 258 (*Heart Circ. Physiol.* 27): H140–H144, 1990.

37. **Vornanen, M., N. Shepherd, and G. Isenberg.** Tension-voltage relations of single myocytes reflect Ca release triggered by Na/Ca exchange at 35°C but not 23°C. *Am. J. Physiol.* 267 (*Cell Physiol.* 36): C623–C632, 1994.
38. **Yelamarty, R. V., R. L. Moore, F. T. S. Yu, M. Elensky, A. M. Semanchick, and J. Y. Cheung.** Relaxation abnormalities in single cardiac myocytes from renovascular hypertensive rats. *Am. J. Physiol.* 262 (*Cell Physiol.* 31): C980–C990, 1992.
39. **Zhang, X.-Q., R. L. Moore, T. Tenhave, and J. Y. Cheung.** $[Ca^{2+}]_i$ transients in hypertensive and postinfarction myocytes. *Am. J. Physiol.* 269 (*Cell Physiol.* 38): C632–C640, 1995.
40. **Zhang, X.-Q., R. L. Moore, D. L. Tillotson, and J. Y. Cheung.** Calcium currents in postinfarction rat cardiac myocytes. *Am. J. Physiol.* 269 (*Cell Physiol.* 38): C1464–C1473, 1995.
41. **Zhang, X.-Q., D. L. Tillotson, R. L. Moore, R. Zelis, and J. Y. Cheung.** Na^+/Ca^{2+} exchange currents and SR Ca^{2+} contents in postinfarction myocytes. *Am. J. Physiol.* 271 (*Cell Physiol.* 40): C1800–C1807, 1996.